Title
Opto-Thermophoretic Tweezers and Assembly.

Journal
Journal of Micro and Nano-Manufacturing, 6(4)

ISSN
2166-0468

Authors
Li, Jingang
Lin, Linhan
Inoue, Yuji
et al.

Publication Date
2018-12-01

DOI
10.1115/1.4041615

Peer reviewed

Jingang Li
Materials Science and Engineering Program
and Department of Mechanical Engineering,
The University of Texas at Austin,
Austin, TX 78712

Linhan Lin
Materials Science and Engineering Program and
Department of Mechanical Engineering,
The University of Texas at Austin,
Austin, TX 78712

Yuji Inoue
Materials Science and Engineering Program and
Department of Mechanical Engineering,
The University of Texas at Austin,
Austin, TX 78712

Yuebing Zheng[1]
Materials Science and Engineering Program and
Department of Mechanical Engineering,
The University of Texas at Austin,
Austin, TX 78712
e-mail: zheng@austin.utexas.edu

Opto-Thermophoretic Tweezers and Assembly

Opto-thermophoretic manipulation is an emerging field, which exploits the thermophoretic migration of particles and colloidal species under a light-controlled temperature gradient field. The entropically favorable photon–phonon conversion and widely applicable heat-directed migration make it promising for low-power manipulation of variable particles in different fluidic environments. By exploiting an optothermal substrate, versatile opto-thermophoretic manipulation of colloidal particles and biological objects can be achieved via optical heating. In this paper, we summarize the working principles, concepts, and applications of the recently developed opto-thermophoretic techniques. Opto-thermophoretic trapping, tweezing, assembly, and printing of colloidal particles and biological objects are discussed thoroughly. With their low-power operation, simple optics, and diverse functionalities, opto-thermophoretic manipulation techniques will offer great opportunities in materials science, nanomanufacturing, life sciences, colloidal science, and nanomedicine. [DOI: 10.1115/1.4041615]

1 Introduction

Optical tweezers, which use optical gradient forces to directly trap colloidal particles at the focused laser beam center, were first proposed by Ashkin in 1970 [1]. Since then, optical tweezers have been extensively applied for trapping and manipulating dielectric particles, plasmonic particles, cells, viruses, and bacteria [2–5]. The development of optical manipulation technology provides an ideal platform to investigate and advance nanotechnological applications in various fields, such as colloidal bonding and interactions, drug deliveries, cells and biomolecules, functional nanodevices, and nanomedicines [6–10]. Despite this far-reaching progress, accurate manipulation of nanometer-sized particles is difficult due to the diffraction limit [2,11]. Additionally, the use of high optical power (10^2–10^3 mW) could damage nanoparticles and biological cells [12,13].

To overcome these limitations, various strategies were proposed. Plasmonic tweezers exploit the localized surface plasmon resonances of metallic nanostructures for near-field trapping [14–17]. The plasmon-enhanced optical forces significantly reduce the required operational power of plasmonic tweezers [18,19]. Additionally, the localized plasmonic hot spots favor the trapping of nanoparticles and molecules beyond the diffraction limits [20]. However, the localized and near-field nature of plasmonic tweezers limits its capability to dynamically manipulate a given sample [21]. An alternative approach to trapping is to harness indirect optomechanical coupling under a light-controlled electric field or temperature field. For instance, optoelectronic tweezers use light to create virtual electrodes and utilize dielectrophoretic forces to manipulate particles under a nonuniform electric field [22,23]. Integrated with a floating electrode, phototransistors, and microfluidics, optoelectronic tweezers have advanced many applications in dynamic cell and particle manipulation [24–26].

Opto-thermophoretic manipulation creates a temperature gradient field through optical heating, exploiting the thermophoretic migration of particles under a temperature field [27,28]. The entropically favorable photon–phonon conversion enables the generation of a strong temperature gradient with low-power optical heating [29]. Furthermore, the universally applicable thermophoretic motion allows for the manipulation of various particles in diverse colloidal systems. This review summarizes recent progress in opto-thermophoretic tweezers and assembly as well as their applications. We first discuss the underlying mechanisms involved in opto-thermophoretic manipulation. Then, we introduce opto-thermophoretic trapping of nano-objects in localized temperature gradients based on thermophoretic migration. Next, we compare the different mechanisms of two opto-thermophoretic tweezers. Entropy-driven thermophoretic tweezers utilize entropy-driven forces created by a permittivity gradient at the particle-solvent interface, and opto-thermoelectric nanotweezers (OTENT) harness the thermophoresis-induced thermoelectric field to manipulate small nanoparticles. Finally, we review the opto-thermophoretic assembly and construction of diverse colloidal matter structures based on opto-thermoelectric tweezers and depletion attraction.

2 Working Mechanisms

Managing particle movements under a laser-generated temperature field is crucial to opto-thermophoretic manipulation. A plethora of experiments have shown the directed thermophoretic migration of particles toward the cold or the hot regions [30–34]. However, thermal gradient induced particle motion is quite complicated, requiring thorough consideration of multiple mechanisms and numerous factors such as interfacial properties, temperature, salinity, particle–particle interaction, and solvent compositions [31,35–39]. In this section, we introduce and briefly discuss the main mechanisms involved in opto-thermophoretic tweezers and assembly, including thermophoresis, depletion, and thermoelectricity.

2.1 Thermophoresis

2.1.1 Basic Description. Thermophoresis, also termed the Soret effect, thermodiffusion, or thermal diffusion, acts as a generalized force on particles and drives them to cold or hot regions

[1]Corresponding author.

Contributed by the Manufacturing Engineering Division of ASME for publication in the Journal of Micro- and Nano-Manufacturing. Manuscript received August 13, 2018; final manuscript received September 16, 2018; published online October 18, 2018. Editor: Nicholas Fang.

under a thermal gradient [40]. The drift velocity of particles is given by

$$\boldsymbol{u} = -D_T \nabla T \tag{1}$$

where D_T is the thermophoretic mobility and ∇T is the temperature gradient. In dilute suspensions, the mass flow J can be defined as $J = -D\nabla c - cD_T\nabla T$, where c is the particle concentration and D is the Brownian diffusion coefficient. A steady-state concentration gradient profile is given by Parola and Piazza [30]

$$\nabla c = -cS_T\nabla T \tag{2}$$

here, $S_T = D_T/D$ is called the Soret coefficient. Since D varies significantly for different components, S_T is regarded as a more general description for thermophoresis. $S_T > 0$ occurs for "thermophobic" particles that move to lower temperatures, while $S_T < 0$ when the particles move to higher temperatures, corresponding to thermophilic behavior (Fig. 1(*a*)).

2.1.2 Experimental Methods. The development of reliable and sensitive optical probing techniques has enabled the extensive experimental studies of particle thermophoresis. One simple but powerful method is called "beam deflection" [41]. When the refractivity of a particle does not exactly match that of a solvent, a refractive index gradient ∇n is created associated with particle concentration gradient ∇c. A laser beam propagating along the optically inhomogeneous medium with a temperature gradient undergoes two angular deflections. First, the propagated beam experiences a rapid change $(\Delta\theta)_{th}$, due to the temperature-induced solvent refractivity change, which is then followed by a much slower deflection change $\Delta\theta_s(t)$, due to the buildup of particle concentration gradient caused by thermophoresis. By analyzing angular deflections and comparing with optical effects on the pure solvent, one can easily obtain the Soret coefficient S_T.

Thermal lensing exploits the self-effect on beam propagation when a focused laser beam increases the temperature of an absorbing medium, generating a locally inhomogeneous refractive-index profile [42–44]. This radial refractivity gradient acts as a negative lens, which increases the divergence of the laser beam. Meanwhile, the laser-induced temperature gradient drives thermophoretic motion, building up a particle concentration gradient within the heated region, which acts as an additional lenslike element. Similar to beam deflection, "thermal" and thermophoretic lensing effects take place on separated timescales, which can be differentiated and further analyzed to evaluate the Soret coefficient. Thermal lensing yields a comparable accuracy to the beam deflection method and is more appropriate for suspensions with high viscosity or larger particle size.

Another all-optical technique uses fluorescent-dyed particles, which allows the laser-induced particle concentration profile to be monitored through the detection of spatial and time dependences of their fluorescent intensities [45]. The key advantage of this fluorescence detection method is that it allows the thermophoretic motion of single colloidal particle to be visualized as long as individual particle emission is resolved. Recently, total internal reflection microscopy based on single particle evanescent light scattering has also been used to study thermophoresis and directly measure thermophoretic forces [46].

2.1.3 Surface Chemistry Dependency. Thermophoresis is a nonequilibrium effect induced by a thermal gradient and depends on interfacial, particle, and solvent properties. In the last two decades, numerous efforts have been made to investigate thermophoresis of particles and to develop theoretical models of the Soret coefficient. Morozov studied thermal diffusion in disperse systems and reported that the sign of Soret coefficient depends on electrostatic surface potential and Debye length [35]. This dependence was further studied by Piazza and Guarino who found that the Soret coefficient is strongly related to the solution ionic strength and the Debye length in sodium dodecyl sulfate (SDS) micellar solution [47]. This strict relation between thermophoresis and the particle–solvent interactions has been further supported in measurements of a mixture of SDS and dodecylmaltoside [48]. Dhont developed a microscopic approach to describe the thermodiffusion of interacting colloids, where sign changes of the Soret coefficient can be expected on variation of concentration and temperature [49,50]. Parola and Piazza proposed to solve the time-dependent density profile of noninteracting spherical colloids under a force density $\boldsymbol{f}$ using the Smoluchowski equation [30]. The net force $\boldsymbol{f}$ due to the presence of a thermal gradient can then be calculated based on hydrodynamic equations and momentum conservation.

2.1.4 Size Dependency. Duhr and Braun showed that thermophoresis can be described with a local thermodynamic equilibrium at moderate temperature gradients [51]. By equating the local Boltzmann law $dc/c = -dG/kT$ with Eq. (2), the Soret coefficient S_T is connected with Gibbs free energy G. By applying the thermodynamic relation, the Soret coefficient can be expressed with the entropy of the particle–solvent system S according to $S_T = -S/kT$ at a constant pressure [33]. The entropy S scales linearly with particle surface area; thus, the Soret coefficient S_T increases linearly over particle surface, that is $S_T \propto a^2$ (a is the particle radius). Since $D \propto a^{-1}$, thermophoretic mobility D_T scales with particle radius as $D_T \propto a$. However, this result was questioned by a number of other reported results [37,38,52], where thermophoretic mobility had no correlation with particle size. Piazza and coworkers performed experiments on colloidal particles with standardized particle–solvent interface and observed a similar D_T for all particle sizes [52]. Similarly, the thermophoretic mobility of high polymers is independent of the molecular weight [53].

2.1.5 Temperature Dependency. Temperature also plays an important role on the Soret coefficient. A sign reversal of S_T has been reported by decreasing temperature, leading to a change from "thermophobic" to "thermophilic" behavior [33,37,41]. The temperature dependence of $S_T(T)$ is generally well described by an empirical fitting function proposed by Iacopini and Piazza [41]

$$ST(T) = S_T^{\infty}\left[1 - \exp\left(\frac{T^* - T}{T_0}\right)\right] \tag{3}$$

where S_T^{∞} represents the high-temperature limit, T^* is the critical temperature where S_T changes sign, and T_0 represents the strength of the temperature effects.

2.1.6 Discussion. Rigorous experimental tests have been performed to study thermophoresis of various suspension systems,

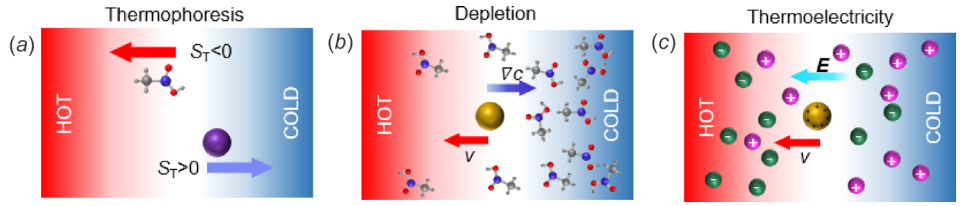

Fig. 1 Schematic illustration for (*a*) thermophoresis, (*b*) depletion, and (*c*) thermoelectricity

including latex particles [52], polymers [53], surfactant aggregates [47], and biological molecules [41,45]. Several successful approaches have been developed to understand the Soret effect of particles, such as temperature and size dependencies [41,52]. Due to the large variations for each system, theoretical models have been mostly developed from specific colloidal systems, and general models of particle thermophoresis in liquids are still lacking. One essential difficulty is to find a universal method to describe the particle–solvent interfacial properties. Additionally, no real external field is present for thermophoresis, which makes it challenging to calculate the force exerted on the particles.

Fundamental investigation of thermophoresis has facilitated the practical applications in many fields. Soret migration offers a noninvasive way to manipulate molecules with a thermal gradient. Braun et al. achieved trapping of DNA through thermophoresis and convection with more than 1000-fold enhanced concentrations [54]. Weinert et al. reported an optical conveyor belt using a bidirectional flow and a thermophoretic drift to transport and trap small molecules at a single spot [55]. Recently, Zhang et al. achieved the size-dependent molecular translocation based on size-dependent thermophoresis of DNA molecules [56]. Besides molecule manipulation, thermophoresis has further been used as a powerful tool to quantify biomolecular interactions, known as MicroScale Thermophoresis [57]. MicroScale Thermophoresis has emerged as a revolutionary technique to monitor the directed movement of fluorescent molecules under microscopic temperature gradients to analyze a variety of biomolecular interactions, ranging from oligonucleotide interactions, protein–DNA interactions, and protein–protein interactions [58].

2.2 Depletion Forces. Depletion forces arise from the thermophoretic migration in hybrid colloidal systems. In a colloid–polymer mixture, in which the particle size is larger than the polymer gyration radius R, the polymers migrate more quickly than particles traveling from the hot to the cold region, forming a concentration gradient, ∇c. Subsequently, the entropic repulsion pushes the particle to lower polymer concentration, i.e., the hot region (Fig. 1(*b*)), with a velocity opposite to ∇c [59]

$$\boldsymbol{u} = -\frac{k_B T R^2}{3\eta}\nabla c \tag{4}$$

where k_B is the Boltzmann constant and η is the solvent viscosity. From Eq. (4), both the concentration and size of the polymer will strongly affect the strength of depletion force. Jiang et al. achieved the trapping of the colloids (beads and DNA molecules) in polyethylene glycol solution by harnessing depletion forces, and the trapped colloid density increased with the polymer concentration [59].

Depletion forces have been widely used to transport, trap, and assemble colloidal particles [60–62]. In addition to polymer molecules, other components such as nanoparticles, micelles, and vesicles can also act as the depletants to control the migration of colloidal particles [63]. For instance, Deng et al. demonstrated the assembly of microspheres (silica or polystyrene beads) into three-dimensional crystals by depletion force produced by magnetic Fe_3O_4 nanoparticles [64]. The Fe_3O_4 nanoparticles were quickly drawn away from the laser spot through both thermophoresis and optical force, generating a nonequilibrium depletion force, which drove the microspheres to the laser spot to form a hexagonal lattice with negligible defects. The tight binding of microspheres makes thermophoretic depletion a low-cost and fast fabrication technique for high-quality three-dimensional (3D) colloidal photonic crystals.

2.3 Thermoelectricity. Under a temperature gradient, the spatial redistribution of the cations and the anions ions in an electrolyte solution generates a thermoelectric field [65]. Depending on their ionic radius and solvation energy, positive and negative ions migrate at different rates and directions under thermophoresis, causing accumulations at different regions. This spatial separation results in a thermoelectric field in a steady-state, and charged colloidal particles drift to either the hot or the cold regions, depending on the sign of its charge (Fig. 1(*c*)).

The presence of a thermoelectric field has strong effects on the thermophoretic motion of colloidal particles. By measuring the effective thermodiffusion coefficient D_T (or Soret coefficient S_T) in electrolyte solutions, thermoelectric effects of different electrolyte systems have been extensively investigated. Putnam and Cahill measured the thermodiffusion coefficient D_T of charged polystyrene spheres in high-concentration salt solution, where D_T for charged latex spheres could be controlled from -0.9×10^{-7} cm^2 s^{-1} K^{-1} to $\sim1.5\times10^{-7}$ cm^2 s^{-1} K^{-1} by changing the ionic species in solution [66]. Würger later studied the transport of charged colloid in the presence of strongly mobile ionic species and showed that the colloid thermophoresis was strongly affected by electrolyte Soret and Seebeck effects [67]

$$D_T = \frac{\xi e^2}{12\eta\varepsilon T}\left[(1+\alpha+\tau)\sigma^2\lambda^2 - \delta\alpha\frac{3\sigma\lambda}{\pi l_B}\right] \tag{5}$$

Here, $\xi = 3\kappa_s/(2\kappa_s + \kappa_p)$ accounts for the thermal conductivity ratio of solvent (κ_s) and particle (κ_p), e is the elemental charge, ε is the solvent permittivity, λ is the Debye length, σ is the surface charge density, $\tau = -\partial\ln\varepsilon/\partial\ln T$, l_B is the Bjerrum length, α and $\delta\alpha$ represent the reduced Soret and Seebeck coefficient of the electrolyte solution, respectively. In the absence of electrolyte, Soret and Seebeck effects ($\alpha = 0 = \delta\alpha$), $D_T > 0$, and Eq. (5) agrees with previous results [30,35,47]. For a sufficiently negative Soret coefficient α, a sign reversal occurs, i.e., $D_T < 0$. These results were further confirmed by Eslahian et al., who found that the Soret coefficient of charged polystyrene particles in electrolyte solution was determined by charge effects, and showed a strong specification effect [39]. Braun and coworkers later quantified the thermoelectric effect in general salt solutions as [32]

$$E_T = \frac{k_B T\nabla T}{e}\frac{\sum_i Z_i n_i S_{Ti}}{\sum_i Z_i^2 n_i} \tag{6}$$

where E_T is the thermally generated electric field, i represents the ionic species, and Z_i, n_i, and S_{Ti} are the charge number, the concentration, and the Soret coefficient of ionic species i, respectively. The direction of thermophoretic motion of charged colloid can be controlled by the addition of electrolytes, providing the opportunity for particle manipulation in microfluidic systems.

3 Opto-Thermophoretic Manipulation and Manufacturing

In Sec. 2, we discussed thermophoresis and the related depletion and thermoelectric effects, and additionally presented the thermophoretic trapping of molecules and particles [33,54,62,64]. In this section, we illustrate the thermophoretic trapping of single nano-objects in a dynamic temperature field. Opto-thermophoretic tweezers based on thermophoresis and thermoelectric effects were further developed for low-power manipulation of single nanoparticles. By harnessing the depletion forces, assembly and printing of arbitrary micro/nanostructures were achieved using colloidal particles as building blocks.

3.1 Thermophoretic Trapping of Nano-Objects. The thermophoretic trapping introduced in Sec. 2.1 is limited to large ensembles of colloids and molecules. Cichos and coworkers first utilized plasmonic nanostructures to produce localized temperature fields to confine individual nano-objects in solution [68]. As shown in Fig. 2(*a*), an expanded laser beam heats a closed gold nanohole structure, resulting in a "hot wall," which confines the particle to the center of the trap. The confinement is directly

related to the Soret coefficient and can be enhanced by increasing the heating power. Besides closed gold nanohole structures, trapping can be achieved with an open patchy gold structure using a dynamic focused heating laser (Fig. 2(*b*)). Due to a more localized temperature field at the patches, the local temperature gradient is increased, resulting in a stable trap for nanoparticles (Fig. 2(*c*)). This dynamic heating strategy can also be used for closed gold structures, giving rise to a much larger temperature gradient and enhancing trapping stability significantly [69]. While steering the particle to the trap center, the heating laser rotation also causes a weak tangential drift velocity that pushes the particle away from the trap. This tangential component is due to the finite rotation speed of laser beam and can be significantly eliminated by increasing the rotation frequency [68,69].

Cichos and coworkers further combined the thermophoretic trap with a feedback mechanism to extend the trapping capabilities [70]. The trap consists of a closed gold structure with a dynamic heating laser (Fig. 2(*d*)). The feedback system is realized by analyzing the position of nano-object in the charge-coupled device image and steering the laser beam at the edge of the gold structure with the assistance of an acousto-optical deflector. In contrast to the steady-state, the feedback controlled trap shows a much larger temperature gradient (Fig. 2(*e*)). The width of the Gaussian position distribution in the feedback mode decreased by a factor of 3.5 when compared to the static heating (see insets in Fig. 2(*e*)), and the trapping stiffness increased by a factor of 12. In addition to trapping particles at the center of the trapping region, offset target, multiple point-like targets, ring-like target, and expanded area target were demonstrated (Fig. 2(*f*)), showing the versatility of the trapping scheme. The performance of the feedback-controlled thermophoretic trap further enables the trapping of single molecules, such as λ-DNA molecules.

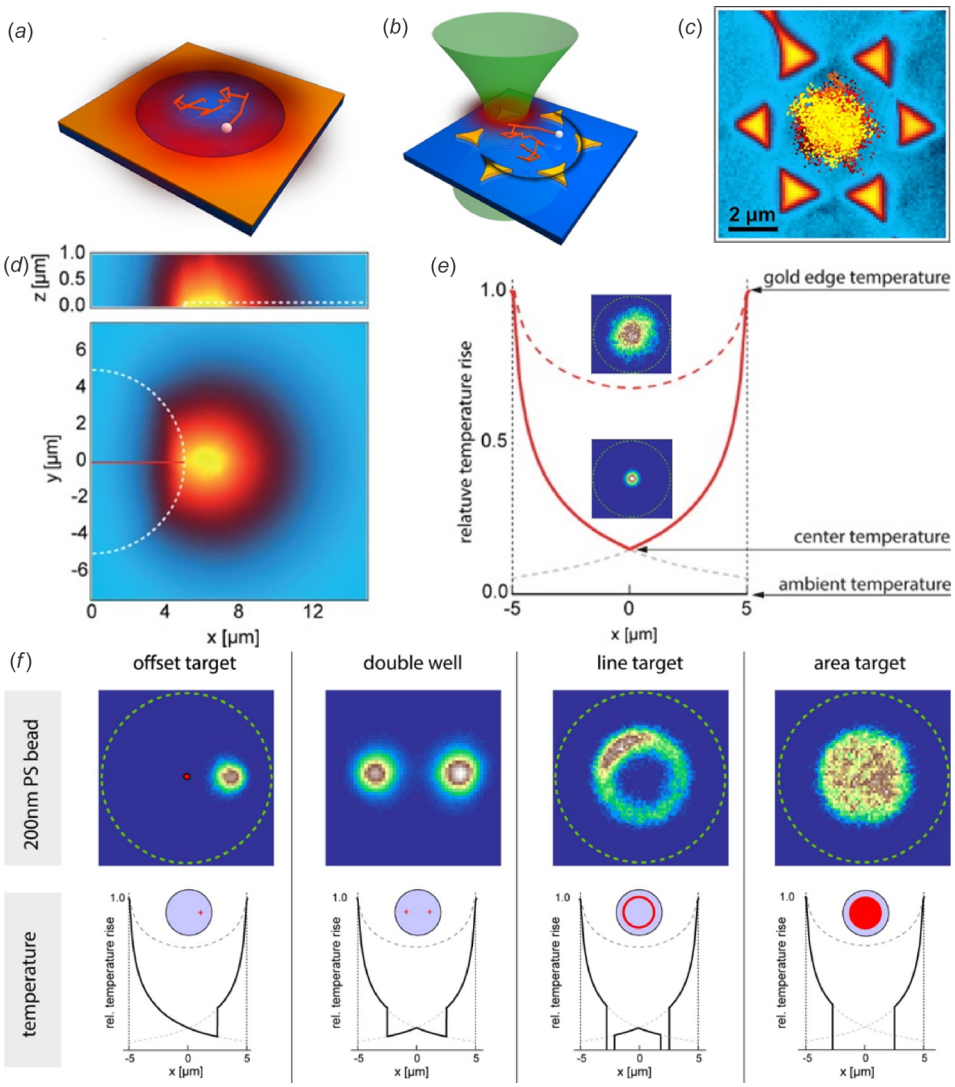

Fig. 2 Thermophoretic trapping of nano-objects by dynamic temperature fields. Thermophoretic trap with (*a*) a closed gold structure and (*b*) an open gold structure with dynamic heating. (*c*) Trajectory points of a 200 nm PS sphere trapped within the open gold structure. (*d*) Calculated temperature map of the relative rise generated by a focused laser beam at the rim of the closed gold structure. (*e*) Calculated relative temperature rise profile (scaled) in the thermophoretic trap at a steady-state (dashed line) and by feedback controlled heating (solid line). The insets show the probability densities of finding a 200 nm polystyrene particle inside the trapping region for a steady-state temperature profile (top) and feedback controlled trapping (bottom) with the same heating power. (*f*) Examples of different effective trapping potential landscapes generated by different feedback rules. (*a*)–(*c*) Reproduced with permission from Braun and Cichos [68], Copyright 2013 by American Chemical Society. (*d*)–(*f*) Reproduced with permission from Braun et al. [70], Copyright 2015 by American Chemical Society.

3.2 Opto-Thermophoretic Tweezers

3.2.1 Entropy-Driven Thermophoretic Tweezers. Thermophoretic trapping using dynamic temperature fields shows the possibility to manipulate single and even multiple macromolecules or particles with well-defined temperature gradients. However, the trapping is limited to an ultrathin water film ($< 1\ \mu$m) and lacks the capability for dynamic manipulation of particles. Lin et al. proposed the thermophoretic tweezers based on entropic responses and permittivity gradients at the particle–solvent interface under an optically generated thermal gradient [71]. The temperature gradient is generated by laser heating of a thermoplasmonic substrate composed of quasi-continuous gold nanoparticles [72–74]. The thermophoretic mobility of the colloidal particle is given by Putnam et al. [37]

$$D_T = -\frac{\varepsilon}{2\eta T}\frac{2\kappa_s}{2\kappa_s+\kappa_p}\left(1+\frac{\partial \ln\varepsilon}{\partial \ln T}\right) \tag{7}$$

where κ_s and κ_p are the thermal conductivities of solvent and particle, respectively. At room temperature, $\tau = \partial \ln\varepsilon / \partial \ln T = -1.4$ in bulk water, resulting in a positive D_T, and thus it is a thermophobic particle. However, in the electric double layer, the permittivity is quite different from the value of bulk water. For charged particles, the polarized water molecules are confined in the electric double layer at the particle surface. The first layer shows a specific orientation due to electrostatic interaction, and the second layer has a loosely oriented structure. The permittivity of these structured water molecules is smaller than that of bulk water, leading to an abnormal permittivity gradient with a positive τ value under thermal perturbation. Therefore, a negative D_T is obtained and the particle drifts from cold to hot regions for trapping *via* optical heating (Fig. 3(*a*)). Thermophoretic tweezers further showed the versatilities for parallel trapping of polystyrene beads with different sizes into various patterns (Fig. 3(*b*)).

Peng et al. recently studied opto-thermophoretic trapping of colloidal particles in various nonionic liquids and reveal that the nonionic driving force originates from a layered structure of solvent molecules at the particle–solvent interface [75]. Molecular dynamics simulations were carried out to validate the mechanism at the molecular level. The trapping efficiency can be enhanced by engineering the particle–solvent interfacial properties, such as the particle hydrophilicity, particle surface charge, and the ionic strength of the solvent.

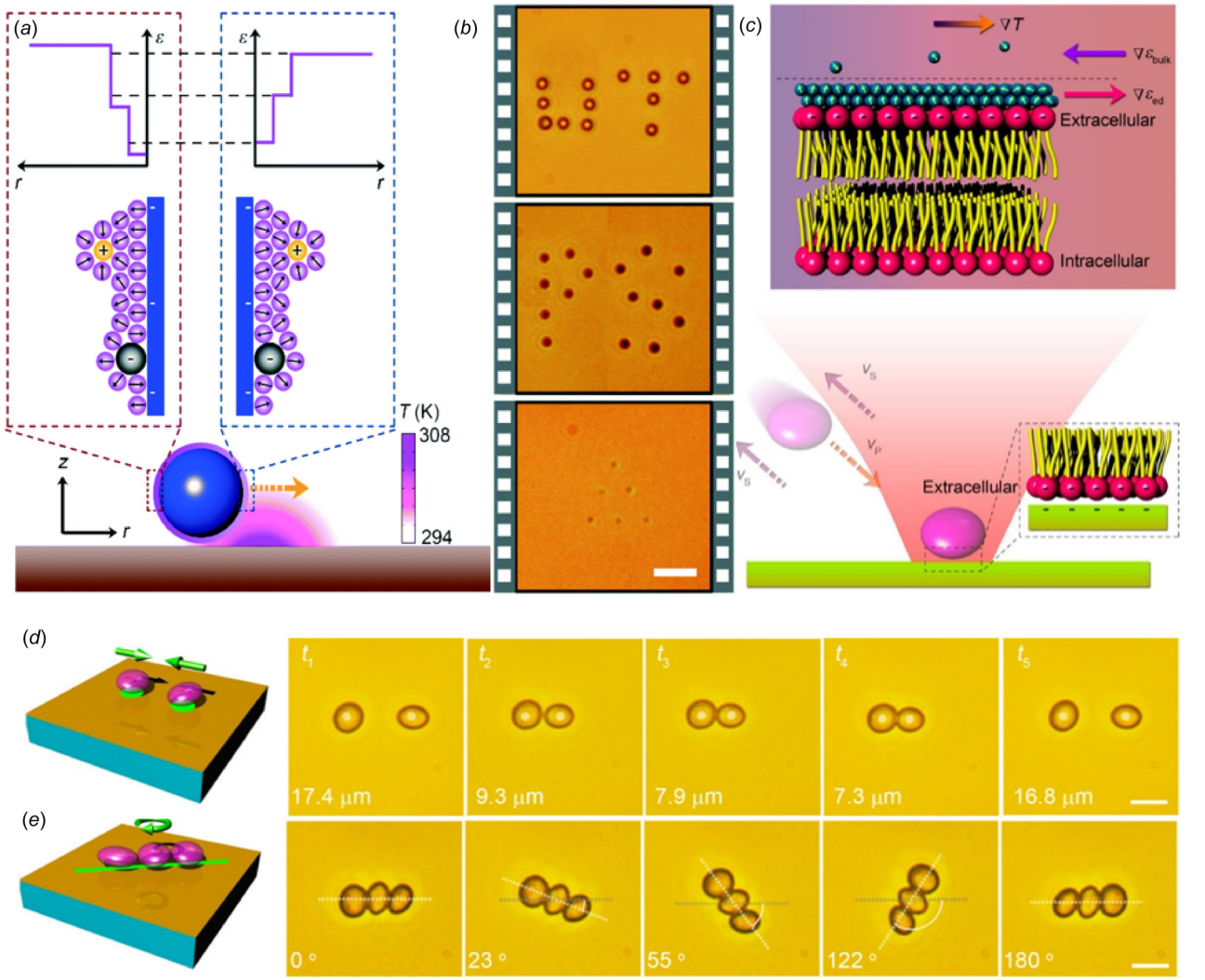

Fig. 3 Entropy-driven thermophoretic tweezers for manipulation of particles and biological cells. (*a*) Schematic showing the working principle of the thermophoretic tweezers. (*b*) Parallel trapping of colloidal particles of different sizes. (*c*) Schematic illustration of the working mechanisms for thermophoretic trapping of biological cells. (*d*) Reversible distance control between a pair of yeast cells. (*e*) Rotation of 1D assembly of three yeast cells. (*a*) and (*b*) Reproduced with permission from Lin et al. [71], Copyright 2017 by The Royal Society of Chemistry. (*c*)–(*e*) Reproduced with permission from Lin et al. [76], Copyright 2017 by American Chemical Society.

Besides colloidal particles, manipulation of biological cells with entropy-driven thermophoretic tweezers has been realized [76]. The phosphate groups in the lipid bilayer provide negative charges on the cell membrane and induce an electric field **E** to drive the water molecules toward the membrane to form the electric double layer structure. The permittivity gradient under a temperature gradient is consistent with the case of charged particle, yielding a negative D_T and trapping cells at the hot laser spot (Fig. 3(*c*)). By integrating the tweezers with a digital micromirror device, versatile manipulation of cells can be achieved. The cell–cell distance can be reversibly controlled at a resolution of 100 nm to tune the intercellular interaction (Fig. 3(*d*)). Precise rotation of 1D cell assembly was also demonstrated to control the orientation at an angular resolution of one degree (Fig. 3(*e*)). Independent rotation of single or multiple yeast cells can be easily achieved as well. In addition to yeast cells, thermophoretic tweezers can be applied for trapping, alignment, and orientation control of highly anisotropic *Escherichia coli* cells.

3.2.2 Opto-Thermoelectric Nanotweezers. Recently, Zheng and coworkers developed the OTENT to capture and manipulate metal nanoparticles at single-particle resolution [77]. A cationic surfactant, cetyltrimethylammonium chloride (CTAC), is added into the solution to enable opto-thermoelectric tweezing. CTAC surfactant coats the particle surface and forms a molecular double layer, leading to a hydrophilic, positively charged surface (Fig. 4(*a*)). Simultaneously, CTAC molecules self-assemble into positive micellar ions above the critical micelle concentration (0.13–0.16 mM) (Fig. 4(*b*)). When a laser beam is directed to a thermoplasmonic substrate, a temperature gradient is generated. Both the CTAC micelles and negative Cl^- migrate from the hot to the cold region by thermophoresis, drifting away from the laser spot. Since S_T (micelle) > S_T (Cl^-), a thermoelectric field pointing toward the laser beam is built due to the spatial separation of CTAC micelles and Cl^- ions, driving the positively charged particle to be trapped by the laser beam (Fig. 4(*c*)). OTENT can trap nanosized metal particles with high trapping stiffness and an extremely low optical power (0.05–0.4 mW μm^{-2}) that is 2–3 orders of magnitude lower than optical tweezers. The trapping capability can be further optimized by tuning the CTAC concentration, which influences the micelle thermophoresis. Integration of a digital micromirror device allows the trapping and

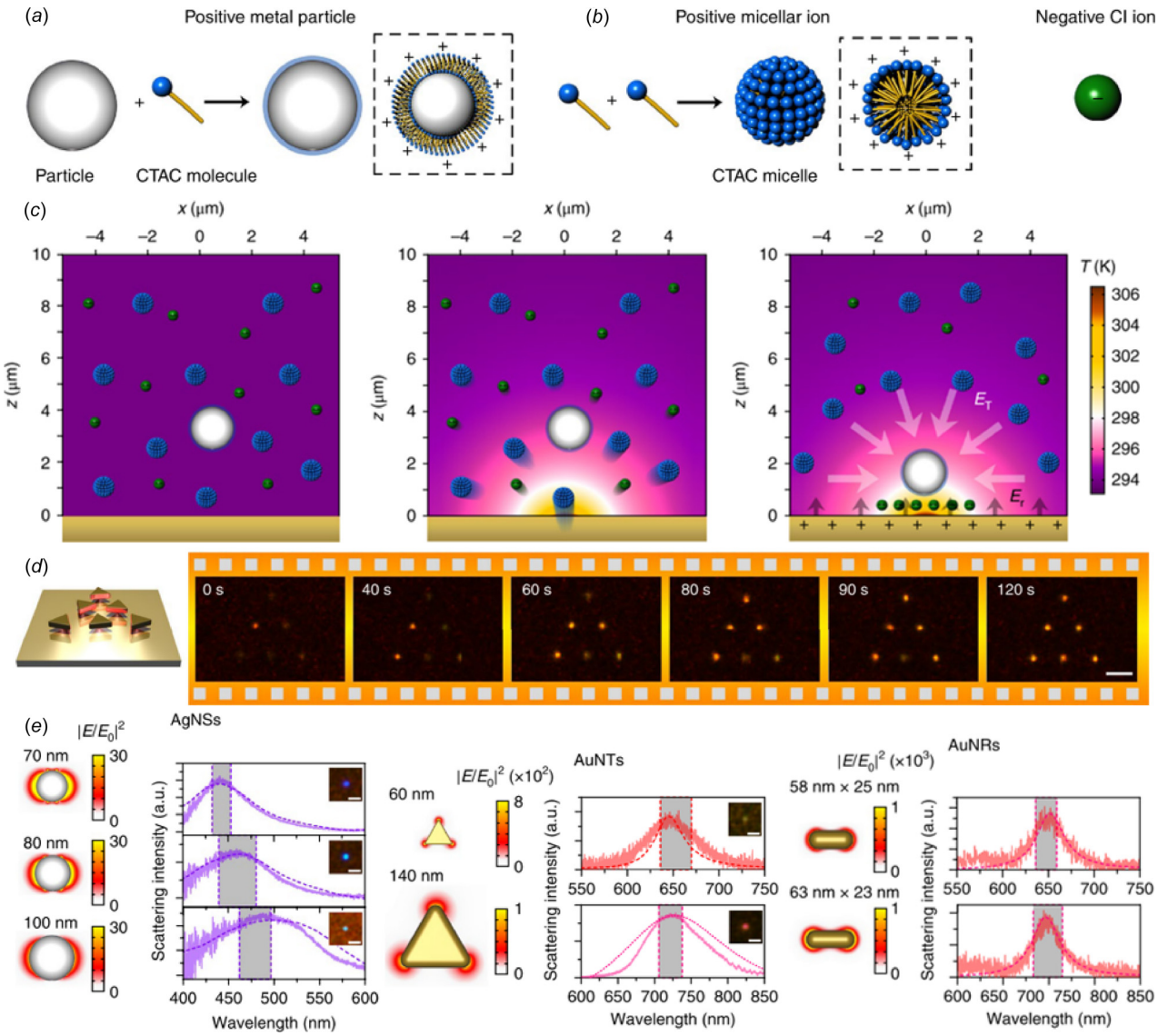

Fig. 4 Opto-thermoelectric nanotweezers. (*a*) Modification of a metal nanoparticle by CTAC adsorption. (*b*) Schematic view of CTAC micelles and Cl^- ions. (*c*) Schematic illustration of working principle of the tweezers. (*d*) Parallel trapping of six 150 nm gold nanotriangles (AuNTs). (*e*) In situ dark-field optical spectroscopy of trapped single metal nanoparticles along with simulated spectra. Reproduced with permission from Lin et al. [77], Copyright 2018 by Springer Nature.

manipulation of multiple metal nanoparticles in parallel using OTENT (Fig. 4(*d*)). Incorporated with a high-performance spectrometer, OTENT also provides the possibility of detecting the intrinsic scattering spectra from the trapped metal particles. Through in situ dark-field scattering spectroscopy, the material, size, and shape of metal nanoparticles can be identified (Fig. 4(*e*)).

Opto-thermophoretic tweezers display the potential to trap wide ranges of colloidal particles and biological cells with a significantly reduced optical intensity compared with optical tweezers. The size limit of metal particles that can be trapped is down to 20 nm. The trapping force arises from optical heating of a thermoplasmonic substrate, which can relax the rigorous optical requirements of optical tweezers. Opto-thermophoretic tweezers further demonstrate versatile particle manipulation capabilities, including parallel trapping, dynamic manipulation, and orientation control.

3.3 Opto-Thermophoretic Assembly and Printing. Light-directed assembly of colloidal nanoparticles offers the possibility to build nanostructures with emerging physical and chemical performances. Lin et al. presented the reversible assembly of plasmonic nanoparticles using plasmon-enhanced thermophoresis at low optical power (Fig. 5(*a*)) [78]. When the laser is on, CTA^+-modified metal nanoparticles migrate from the cold to the hot region in the light-induced temperature-gradient field (Fig. 5(*b*)). Once the nanoparticles are in close contact within the assembly, the van der Waals attraction becomes strong enough to stabilize the assembly. When the laser is off, the repulsive electrostatic force between the positive CTAC molecules leads to the disassembly process (Fig. 5(*c*)). Parallel manipulation of multiple particle assemblies can be achieved by using a spatial light modulator to dynamically control the laser beam in an arbitrary manner (Figs. 5(*d*) and 5(*e*)). This technique is applicable for a wide range of plasmonic nanoparticles with different materials, sizes, and shapes. Due to the strong interparticle plasmonic coupling, assemblies of metal nanoparticles are promising for in situ analysis of target molecules using surface-enhanced Raman spectroscopy (SERS). A detection limit of 1 μM for rhodamine 6G using the 100 nm AgNS assemblies was demonstrated (Fig. 5(*f*)). The SERS sensitivity can be further enhanced by drying the nanoparticle assemblies or using multiple nanoparticle assemblies.

Lin et al. further demonstrated the opto-thermophoretic assembly of colloidal particles into arbitrary configurations (Fig. 6(*a*)) [79]. Colloidal particles of different sizes and materials serve as building blocks. CTAC is added to enable the opto-thermoelectric trapping and manipulation of these building blocks. Meanwhile, CTAC micelles act as depletants, which are driven outside the interparticle gap of two particles, generating a depletion attraction force to bind the colloidal assembly. After the laser is turned off, the assembly can be maintained if the van der Waals interaction and osmotic pressure can overcome the electrostatic repulsive interaction (Fig. 6(*b*)). Diverse colloidal superstructures composed of colloidal particles with various materials, sizes, and shapes can be precisely built using opto-thermophoretic assembly. Several examples including one-dimensional hybrid chain, two-dimensional (2D) hybrid lattice, 2D heptamer with anisotropic tips and various 3D structures are presented in Fig. 6(*c*).

Peng et al. further demonstrated the opto-thermophoretic assembly of diverse colloidal matter superstructures in photocurable hydrogels. The assembled superstructures can be immobilized and patterned on substrates through ultraviolet (UV) cross-linking (Figs. 7(*a*) and 7(*b*)) [80]. The as-built colloidal structures remain intact even after the samples are rinsed and dried, confirmed by the corresponding scanning electron micrograph (Fig. 7(*c*)).

Finally, reconfigurable opto-thermoelectric printing of colloidal particles via light-controlled thermoelectric fields was developed [81]. In this method, NaCl is added to the solution to create the thermoelectric field by the spatial separation of Na^+ and Cl^- ions due to the different Soret coefficients (i.e., S_T (Na^+) > S_T (Cl^-)). The CTAC-functionalized PS spheres are initially trapped by the thermoelectric forces (Fig. 8(*a*)). Then, the spheres are printed *via* depletion attraction induced by the depletion of the CTAC micelles at the particle–substrate interface due to the optical power increase. The particle–substrate bonding is quite strong, causing the printed pattern to remain even after the substrate is rinsed and dried. Arbitrary patterns can be printed with

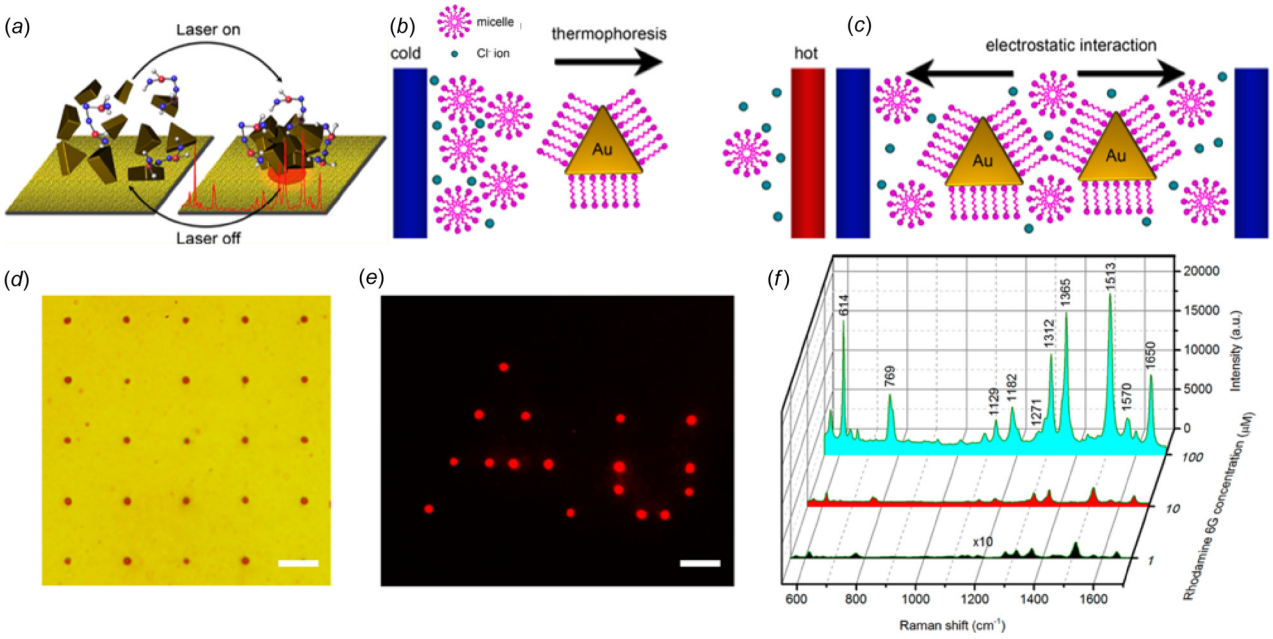

Fig. 5 Reversible assembly of plasmonic nanoparticles. (*a*) Schematic of the light-directed reversible assembly of AuNTs. (*b*) Schematic illustration of the migration of a CTA^+-modified AuNT from cold to hot region. (*b*) Schematic illustration of the release or redispersion of an AuNT assembly due to electrostatic repulsive interaction. (*d*) Optical image of 25 AuNT assemblies in a 5 × 5 square array. (*e*) Dark-field optical image of 17 AuNT assemblies in an Au pattern. (*f*) SERS spectra recorded from single AgNS assemblies for different concentrations of rhodamine 6G. Reproduced with permission from Lin et al. [78], Copyright 2016 by American Chemical Society.

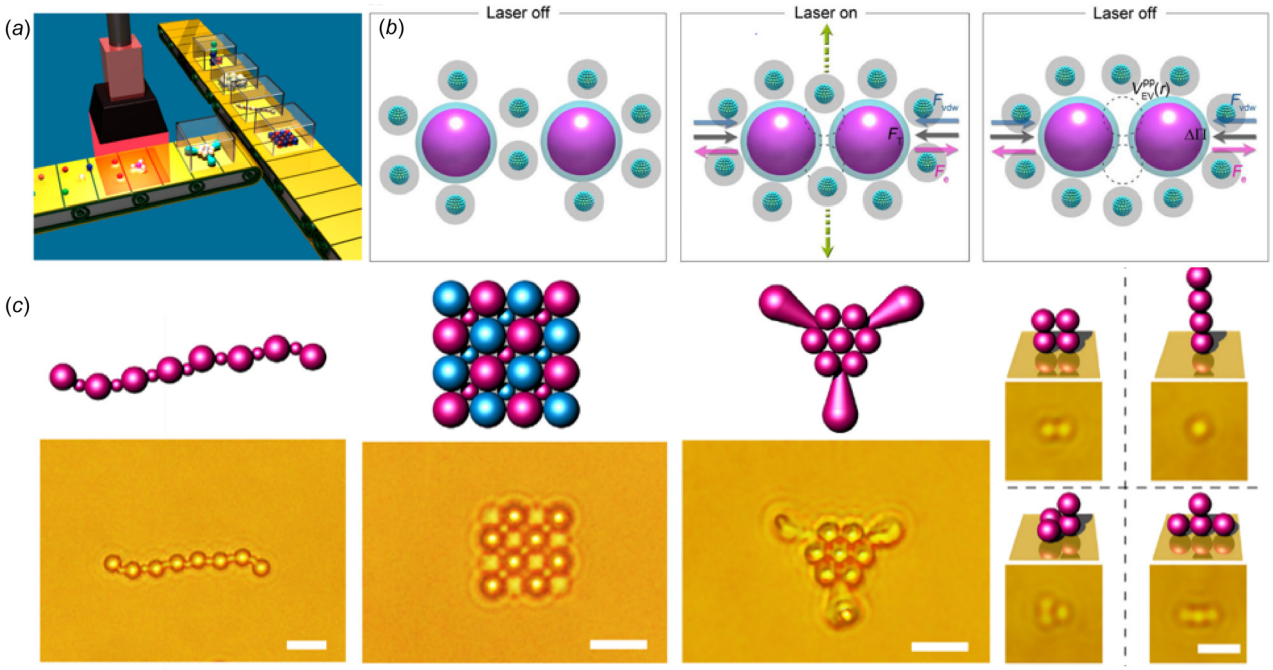

Fig. 6 Opto-thermophoretic assembly of colloidal matter. (*a*) Schematic illustration of the assembly process. (*b*) Illustration of interparticle bonding in assembled structure. (*c*) Diverse types of colloidal structures built by opto-thermophoretic assembly. Reproduced with permission from Lin et al. [79], Copyright 2017 by American Association for the Advancement of Science.

opto-thermoelectric printing, and Fig. 8(*b*) is shown as an example of a "TMI" pattern. By putting the laser beam back to the center of printed particle, the CTAC micelles can be driven back within the particle–substrate gap. The repulsive electrostatic force between the CTAC micelles and the CTAC-coated particles results in the releasing of particles. Reconfigurable printing is achieved by selectively releasing and reprinting one of the printed colloidal particles to realize the transformation from a "sad"-face pattern into a "smiley"-face pattern (Figs. 8(*c*) and 8(*d*)).

Opto-thermophoretic assembly techniques provide a simple and reliable way to construct colloidal superstructures with low optical power. Diverse structures can be readily fabricated with various colloidal particles with a wider range of materials, sizes, and shapes as building blocks. The wide applicability of opto-thermophoretic assembly makes it a useful tool for the fabrication of functional colloidal nanomaterials and devices. Furthermore, the precise control of colloidal assembly configuration and interparticle interaction allows for the tunability of coupling between colloidal atoms and the functions of the assemblies.

4 Conclusion and Outlook

The directed migration of colloids under a temperature gradient, i.e., thermophoresis, has been demonstrated as a promising strategy for trapping, concentrating, and transporting colloidal particles and molecules. Thermophoresis has been widely studied in numerous suspension systems, such as latex particles, polymers, and biomolecules. However, the general principle is still unclear. Future applications will surely benefit from further investigations of the underlying mechanisms of thermophoresis.

Opto-thermophoretic techniques, which exploit the photon–phonon conversion through optical heating and heat-directed particle migration, allow versatile and precise manipulation of colloidal particles, molecules, and biological cells. Compared to conventional optical tweezers, opto-thermophoretic tweezers feature simpler optics, lower optical power, and more applicability. Opto-thermophoretic assemblies have shown the capability to fabricate arbitrary superstructures with a wide range of colloidal particles. Furthermore, the ability to pattern colloidal structures on substrates through either the photopolymerization of hydrogels or the particle–substrate interactions makes it a powerful manufacturing technique for micro- and nano-scale functional devices.

The key of opto-thermophoretic manipulation is to manage light-controlled temperature gradients. Future developments can be realized based on effective substrate engineering and heating optics optimization. In general, any optothermal-responsive material, which can provide a localized temperature field, is suitably applied for opto-thermophoretic manipulation. Thus, optothermal substrates with high photon–phonon conversion efficiency and low thermal conductivities are desired to further reduce the required optical power and improve the optothermal manipulation efficiency. In addition, the use of prepatterned substrates or near-field optics will enable opto-thermophoretic trapping and manipulation with nanoscale precision. Using a femtosecond laser as a heating source would further limit both heat transfer and collective heating on the substrates, improving the temperature gradient for opto-thermophoretic trapping. It is also interesting to design complex particles such as Janus particles with controlled optical, thermal, or electric responses at different regions. The opto-thermophoretic manipulation of these particles could provide

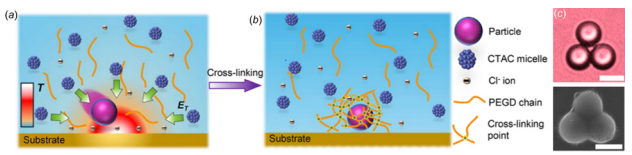

Fig. 7 Opto-thermophoretic construction of colloidal superstructures in photocurable hydrogels. Schematic illustration of (*a*) trapping of a colloidal particle in a thermoelectric field and (*b*) immobilization of the trapped colloidal particle through UV cross-linking. (*c*) Opto-thermophoretic patterning of 2D close-packed superstructures. The bottom image shows the scanning electron micrograph of the corresponding superstructure after cross-linking of the hydrogel. Reproduced with permission from Peng et al. [80], Copyright 2018 by American Chemical Society.

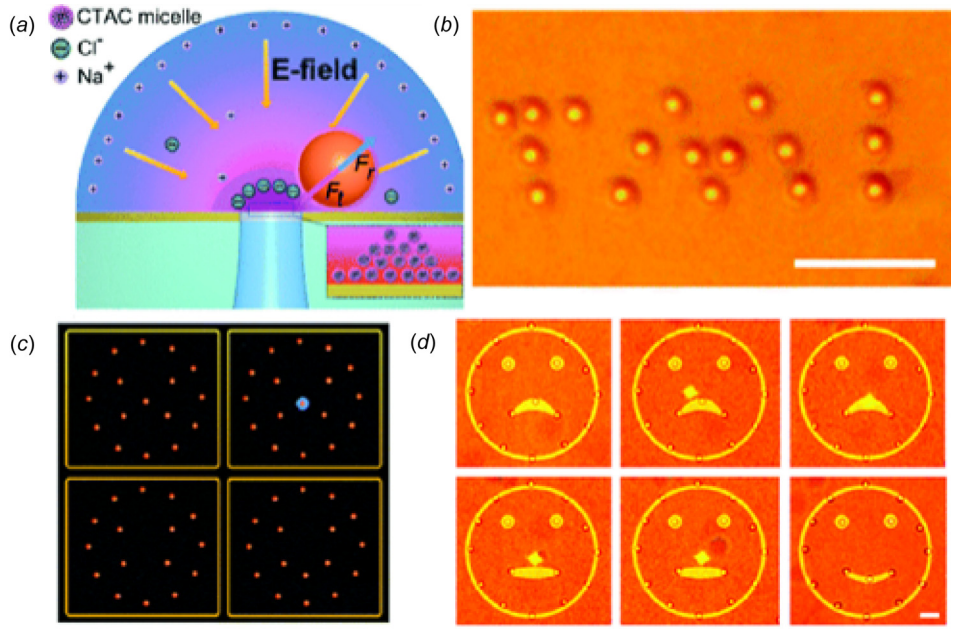

Fig. 8 Opto-thermoelectric printing: (*a*) schematic illustration of the opto-thermoelectric trapping, (*b*) A bright-field optical image of printed TMI pattern of 1 μm PS spheres on the substrate. (*c*) Schematics, and (*d*) optical images of the reconfigurable printing of a sad-face pattern into a smiley-face pattern consisting of 2 μm PS spheres. Reproduced with permission from Lin et al. [81], Copyright 2017 The Royal Society of Chemistry.

distinctive manipulation scenarios and functionalities. Finally, the capability for noninvasive manipulation of biological cells and molecules will bring revolutionary progress in life sciences, disease diagnostics, and nanomedicine.

In addition to manipulating the various species, one of the most promising applications of optothermal techniques is the assembly of functional colloidal structures and devices. The techniques have advantages in their precise control of nanoparticle positions and spatial arrangements on substrates with on-demand reconfigurability, which is promising as a complementary method for on-chip device fabrication. Examples include site-specific creation of single or clusters of metal nanoparticles (or quantum dots) as functional cavities (or emitters) on lithographically fabricated photonic crystals. With their versatile assembly of the variable colloidal nanoparticles, the optothermal techniques can also be applied to fabricate a wide range of functional devices such as colloidal waveguides, sensors, and lasers from bottom up. For the scalable manufacturing of functional materials and devices, one should improve the throughput of current opto-thermophoretic techniques. One of the most promising directions for the throughput improvement is to use a digital micromirror device or a spatial light modulator to multiply working laser beams for parallel operation of colloidal construction and to further exploit well-developed microfluidics for continuous operation with automation. So far, opto-thermophoretic assembly has proved powerful for the construction of 2D superstructures, while its ability to build 3D assemblies is still limited. This limitation can be addressed by using optical fibers coated with optothermal layers to achieve arbitrary 3D manipulation. With its low-power, versatile, and noninvasive operation, opto-thermophoretic assemblies will serve as an emerging nanomanufacturing technique for numerous applications in colloidal sciences, functional nanomaterials and devices, light–matter interaction, and life sciences.

Funding Data

- National Science Foundation (NSF-CMMI-1761743).
- Army Research Office (W911NF-17-1-0561).
- National Aeronautics and Space Administration Early Career Faculty Award (80NSSC17K0520).
- National Institute of General Medical Sciences of the National Institutes of Health (DP2GM128446).

References

[1] Ashkin, A., 1970, "Acceleration and Trapping of Particles by Radiation Pressure," Phys. Rev. Lett., **24**(4), pp. 156–159.
[2] Ashkin, A., Dziedzic, J. M., Bjorkholm, J. E., and Chu, S., 1986, "Observation of a Single-Beam Gradient Force Optical Trap for Dielectric Particles," Opt. Lett., **11**(5), pp. 288–290.
[3] Urban, A. S., Carretero-Palacios, S., Lutich, A. A., Lohmuller, T., Feldmann, J., and Jackel, F., 2014, "Optical Trapping and Manipulation of Plasmonic Nanoparticles: Fundamentals, Applications, and Perspectives," Nanoscale, **6**(9), pp. 4458–4474.
[4] Ashkin, A., Dziedzic, J. M., and Yamane, T., 1987, "Optical Trapping and Manipulation of Single Cells Using Infrared Laser Beams," Nature, **330**(6150), pp. 769–771.
[5] Ashkin, A., and Dziedzic, J., 1987, "Optical Trapping and Manipulation of Viruses and Bacteria," Science, **235**(4795), pp. 1517–1520.
[6] Burns, M. M., Fournier, J.-M., and Golovchenko, J. A., 1989, "Optical Binding," Phys. Rev. Lett., **63**(12), pp. 1233–1236.
[7] Mohanty, S. K., Andrews, J. T., and Gupta, P. K., 2004, "Optical Binding Between Dielectric Particles," Opt. Express, **12**(12), pp. 2746–2753.
[8] Leung, S. J., and Romanowski, M., 2012, "Molecular Catch and Release: Controlled Delivery Using Optical Trapping With Light-Responsive Liposomes," Adv. Mater., **24**(47), pp. 6380–6383.
[9] Maragò, O. M., Jones, P. H., Gucciardi, P. G., Volpe, G., and Ferrari, A. C., 2013, "Optical Trapping and Manipulation of Nanostructures," Nat. Nanotechnol., **8**(11), pp. 807–819.
[10] Applegate, R. W., Squier, J., Vestad, T., Oakey, J., and Marr, D. W. M., 2004, "Optical Trapping, Manipulation, and Sorting of Cells and Colloids in Microfluidic Systems With Diode Laser Bars," Opt. Express, **12**(19), pp. 4390–4398.
[11] Grigorenko, A. N., Roberts, N. W., Dickinson, M. R., and Zhang, Y., 2008, "Nanometric Optical Tweezers Based on Nanostructured Substrates," Nat. Photonics, **2**(6), pp. 365–370.
[12] Babynina, A., Fedoruk, M., Kühler, P., Meledin, A., Döblinger, M., and Lohmüller, T., 2016, "Bending Gold Nanorods With Light," Nano Lett., **16**(10), pp. 6485–6490.
[13] Rasmussen, M. B., Oddershede, L. B., and Siegumfeldt, H., 2008, "Optical Tweezers Cause Physiological Damage to Escherichia Coli and Listeria Bacteria," Appl. Environ. Microbiol., **74**(8), pp. 2441–2446.
[14] Odom, T. W., and Schatz, G. C., 2011, "Introduction to Plasmonics," Chem. Rev., **111**(6), pp. 3667–8.
[15] Ozbay, E., 2006, "Plasmonics: Merging Photonics and Electronics at Nanoscale Dimensions," Science, **311**(5758), pp. 189–193.

[16] Lindquist, N. C., Nagpal, P., McPeak, K. M., Norris, D. J., and Oh, S. H., 2012, "Engineering Metallic Nanostructures for Plasmonics and Nanophotonics," Rep. Prog. Phys, **75**(3), p. 036501.
[17] Juan, M. L., Righini, M., and Quidant, R., 2011, "Plasmon Nano-Optical Tweezers," Nat. Photonics, **5**(6), pp. 349–356.
[18] Yoo, D., Gurunatha, K. L., Choi, H.-K., Mohr, D. A., Ertsgaard, C. T., Gordon, R., and Oh, S.-H., 2018, "Low-Power Optical Trapping of Nanoparticles and Proteins With Resonant Coaxial Nanoaperture Using 10 Nm Gap," Nano Lett., **18**(6), pp. 3637–3642.
[19] Huft, P. R., Kolbow, J. D., Thweatt, J. T., and Lindquist, N. C., 2017, "Holographic Plasmonic Nanotweezers for Dynamic Trapping and Manipulation," Nano Lett., **17**(12), pp. 7920–7925.
[20] Shoji, T., and Tsuboi, Y., 2014, "Plasmonic Optical Tweezers Toward Molecular Manipulation: Tailoring Plasmonic Nanostructure, Light Source, and Resonant Trapping," J. Phys. Chem. Lett., **5**(17), pp. 2957–2967.
[21] Zheng, Y., Ryan, J., Hansen, P., Cheng, Y. T., Lu, T. J., and Hesselink, L., 2014, "Nano-Optical Conveyor Belt—Part II: Demonstration of Handoff Between Near-Field Optical Traps," Nano Lett., **14**(6), pp. 2971–6.
[22] Chiou, P. Y., Ohta, A. T., and Wu, M. C., 2005, "Massively Parallel Manipulation of Single Cells and Microparticles Using Optical Images," Nature, **436**(7049), pp. 370–2.
[23] Wu, M. C., 2011, "Optoelectronic Tweezers," Nat. Photonics, **5**(6), pp. 322–324.
[24] Park, S., Pan, C., Wu, T.-H., Kloss, C., Kalim, S., Callahan, C. E., Teitell, M., and Chiou, E. P. Y., 2008, "Floating Electrode Optoelectronic Tweezers: Light-Driven Dielectrophoretic Droplet Manipulation in Electrically Insulating Oil Medium," Appl. Phys. Lett., **92**(15), p. 151101.
[25] Hsu, H-y., Ohta, A. T., Chiou, P.-Y., Jamshidi, A., Neale, S. L., and Wu, M. C., 2010, "Phototransistor-Based Optoelectronic Tweezers for Dynamic Cell Manipulation in Cell Culture Media," Lab Chip, **10**(2), pp. 165–172.
[26] Huang, K.-W., Wu, Y.-C., Lee, J.-A., and Chiou, P.-Y., 2013, "Microfluidic Integrated Optoelectronic Tweezers for Single-Cell Preparation and Analysis," Lab Chip, **13**(18), pp. 3721–3727.
[27] Lin, L., Hill, E. H., Peng, X., and Zheng, Y., 2018, "Optothermal Manipulations of Colloidal Particles and Living Cells," Acc. Chem. Res., **51**(6), pp. 1465–1474.
[28] Zhao, C., Xie, Y., Mao, Z., Zhao, Y., Rufo, J., Yang, S., Guo, F., Mai, J. D., and Huang, T. J., 2014, "Theory and Experiment on Particle Trapping and Manipulation Via Optothermally Generated Bubbles," Lab Chip, **14**(2), pp. 384–391.
[29] Xie, Y., and Zhao, C., 2017, "An Optothermally Generated Surface Bubble and Its Applications," Nanoscale, **9**(20), pp. 6622–6631.
[30] Parola, A., and Piazza, R., 2004, "Particle Thermophoresis in Liquids," Eur. Phys. J. E, **15**(3), pp. 255–263.
[31] Piazza, R., and Parola, A., 2008, "Thermophoresis in Colloidal Suspensions," J. Phys.: Condens. Matter, **20**(15), p. 153102.
[32] Reichl, M., Herzog, M., Götz, A., and Braun, D., 2014, "Why Charged Molecules Move Across a Temperature Gradient: The Role of Electric Fields," Phys. Rev. Lett., **112**(19), p. 198101.
[33] Duhr, S., and Braun, D., 2006, "Why Molecules Move along a Temperature Gradient," Proc. Natl. Acad. Sci. U. S. A, **103**(52), pp. 19678–19682.
[34] Piazza, R., 2008, "Thermophoresis: Moving Particles With Thermal Gradients," Soft Matter, **4**(9), pp. 1740–1744.
[35] Morozov, K. I., 1999, "Thermal Diffusion in Disperse Systems," J. Exp. Theor. Phys., **88**(5), pp. 944–946.
[36] Julien, M., and Alois, W., 2009, "Thermophoresis at a Charged Surface: The Role of Hydrodynamic Slip," J. Phys.: Condens. Matter, **21**(3), p. 035103.
[37] Putnam, S. A., Cahill, D. G., and Wong, G. C. L., 2007, "Temperature Dependence of Thermodiffusion in Aqueous Suspensions of Charged Nanoparticles," Langmuir, **23**(18), pp. 9221–9228.
[38] Vigolo, D., Brambilla, G., and Piazza, R., 2007, "Thermophoresis of Microemulsion Droplets: Size Dependence of the Soret Effect," Phys. Rev. E, **75**(Pt 1), p. 040401.
[39] Eslahian, K. A., Majee, A., Maskos, M., and Würger, A., 2014, "Specific Salt Effects on Thermophoresis of Charged Colloids," Soft Matter, **10**(12), pp. 1931–1936.
[40] Roberto, P., 2004, "Thermal Forces': Colloids in Temperature Gradients," J. Phys.: Condens. Matter, **16**(38), p. S4195.
[41] Iacopini, S., and Piazza, R., 2003, "Thermophoresis in Protein Solutions," EPL Europhys. Lett., **63**(2), p. 247.
[42] Gordon, J. P., Leite, R. C. C., Moore, R. S., Porto, S. P. S., and Whinnery, J. R., 1965, "Long-Transient Effects in Lasers With Inserted Liquid Samples," J. Appl. Phys., **36**(1), pp. 3–8.
[43] Rusconi, R., Isa, L., and Piazza, R., 2004, "Thermal-Lensing Measurement of Particle Thermophoresis in Aqueous Dispersions," J. Opt. Soc. Am. B, **21**(3), pp. 605–616.
[44] Giglio, M., and Vendramini, A., 1974, "Thermal Lens Effect in a Binary Liquid Mixture: A New Effect," Appl. Phys. Lett., **25**(10), pp. 555–557.
[45] Duhr, S., Arduini, S., and Braun, D., 2004, "Thermophoresis of DNA Determined by Microfluidic Fluorescence," Eur. Phys. J. E, **15**(3), pp. 277–286.
[46] Helden, L., Eichhorn, R., and Bechinger, C., 2015, "Direct Measurement of Thermophoretic Forces," Soft Matter, **11**(12), pp. 2379–2386.
[47] Piazza, R., and Guarino, A., 2002, "Soret Effect in Interacting Micellar Solutions," Phys. Rev. Lett., **88**(20), p. 208302.
[48] Iacopini, S., Rusconi, R., and Piazza, R., 2006, "The "Macromolecular Tourist": Universal Temperature Dependence of Thermal Diffusion in Aqueous Colloidal Suspensions," Eur. Phys. J. E, **19**(1), pp. 59–67.
[49] Dhont, J. K. G., 2004, "Thermodiffusion of Interacting Colloids—I: A Statistical Thermodynamics Approach," J. Chem. Phys., **120**(3), pp. 1632–1641.
[50] Dhont, J. K. G., 2004, "Thermodiffusion of Interacting Colloids—II: A Microscopic Approach," J. Chem. Phys., **120**(3), pp. 1642–1653.
[51] Duhr, S., and Braun, D., 2006, "Thermophoretic Depletion Follows Boltzmann Distribution," Phys. Rev. Lett., **96**(16), p. 168301.
[52] Braibanti, M., Vigolo, D., and Piazza, R., 2008, "Does Thermophoretic Mobility Depend on Particle Size?," Phys. Rev. Lett., **100**(10), p. 108303.
[53] Wiegand, S., 2004, "Thermal Diffusion in Liquid Mixtures and Polymer Solutions," J. Phys.: Condens. Matter, **16**(10), p. R357.
[54] Braun, D., and Libchaber, A., 2002, "Trapping of DNA by Thermophoretic Depletion and Convection," Phys. Rev. Lett., **89**(18), p. 188103.
[55] Weinert, F. M., and Braun, D., 2009, "An Optical Conveyor for Molecules," Nano Lett., **9**(12), pp. 4264–4267.
[56] Zhang, M., Ngampeerapong, C., Redin, D., Ahmadian, A., Sychugov, I., and Linnros, J., 2018, "Thermophoresis-Controlled Size-Dependent DNA Translocation Through an Array of Nanopores," ACS Nano, **12**(5), pp. 4574–4582.
[57] Wienken, C. J., Baaske, P., Rothbauer, U., Braun, D., and Duhr, S., 2010, "Protein-Binding Assays in Biological Liquids Using Microscale Thermophoresis," Nat. Commun, **1**(7), p. 100.
[58] Jerabek-Willemsen, M., André, T., Wanner, R., Roth, H. M., Duhr, S., Baaske, P., and Breitsprecher, D., 2014, "Microscale Thermophoresis: Interaction Analysis and Beyond," J. Mol. Struct., **1077**, pp. 101–113.
[59] Jiang, H.-R., Wada, H., Yoshinaga, N., and Sano, M., 2009, "Manipulation of Colloids by a Nonequilibrium Depletion Force in a Temperature Gradient," Phys. Rev. Lett., **102**(20), p. 208301.
[60] Anderson, J. L., and Prieve, D. C., 1984, "Diffusiophoresis: Migration of Colloidal Particles in Gradients of Solute Concentration," Sep. Purif. Methods, **13**(1), pp. 67–103.
[61] Zhao, K., and Mason, T. G., 2007, "Directing Colloidal Self-Assembly Through Roughness-Controlled Depletion Attractions," Phys. Rev. Lett., **99**(26), p. 268301.
[62] Baranov, D., Fiore, A., van Huis, M., Giannini, C., Falqui, A., Lafont, U., Zandbergen, H., Zanella, M., Cingolani, R., and Manna, L., 2010, "Assembly of Colloidal Semiconductor Nanorods in Solution by Depletion Attraction," Nano Lett., **10**(2), pp. 743–749.
[63] Edwards, T. D., and Bevan, M. A., 2012, "Depletion-Mediated Potentials and Phase Behavior for Micelles, Macromolecules, Nanoparticles, and Hydrogel Particles," Langmuir, **28**(39), pp. 13816–13823.
[64] Deng, H.-D., Li, G.-C., Liu, H.-Y., Dai, Q.-F., Wu, L.-J., Lan, S., Gopal, A. V., Trofimov, V. A., and Lysak, T. M., 2012, "Assembling of Three-Dimensional Crystals by Optical Depletion Force Induced by a Single Focused Laser Beam," Opt. Express, **20**(9), pp. 9616–9623.
[65] Majee, A., and Würger, A., 2012, "Charging of Heated Colloidal Particles Using the Electrolyte Seebeck Effect," Phys. Rev. Lett., **108**(11), p. 118301.
[66] Putnam, S. A., and Cahill, D. G., 2005, "Transport of Nanoscale Latex Spheres in a Temperature Gradient," Langmuir, **21**(12), pp. 5317–5323.
[67] Würger, A., 2008, "Transport in Charged Colloids Driven by Thermoelectricity," Phys. Rev. Lett., **101**(10), p. 108302.
[68] Braun, M., and Cichos, F., 2013, "Optically Controlled Thermophoretic Trapping of Single Nano-Objects," ACS Nano, **7**(12), pp. 11200–11208.
[69] Braun, M., Wurger, A., and Cichos, F., 2014, "Trapping of Single Nano-Objects in Dynamic Temperature Fields," Phys. Chem. Chem. Phys., **16**(29), pp. 15207–15213.
[70] Braun, M., Bregulla, A. P., Günther, K., Mertig, M., and Cichos, F., 2015, "Single Molecules Trapped by Dynamic Inhomogeneous Temperature Fields," Nano Lett., **15**(8), pp. 5499–5505.
[71] Lin, L., Peng, X., Mao, Z., Wei, X., Xie, C., and Zheng, Y., 2017, "Interfacial-Entropy-Driven Thermophoretic Tweezers," Lab Chip, **17**(18), pp. 3061–3070.
[72] Kang, Z., Chen, J., Wu, S.-Y., Chen, K., Kong, S.-K., Yong, K.-T., and Ho, H.-P., 2015, "Trapping and Assembling of Particles and Live Cells on Large-Scale Random Gold Nano-Island Substrates," Sci. Rep., **5**, p. 9978.
[73] Lin, L., Peng, X., Mao, Z., Li, W., Yogeesh, M. N., Rajeeva, B. B., Perillo, E. P., Dunn, A. K., Akinwande, D., and Zheng, Y., 2016, "Bubble-Pen Lithography," Nano Lett., **16**(1), pp. 701–708.
[74] Chen, J., Cong, H., Loo, F.-C., Kang, Z., Tang, M., Zhang, H., Wu, S.-Y., Kong, S.-K., and Ho, H.-P., 2016, "Thermal Gradient Induced Tweezers for the Manipulation of Particles and Cells," Sci. Rep., **6**, p. 35814.
[75] Peng, X., Lin, L., Hill, E. H., Kunal, P., Humphrey, S. M., and Zheng, Y., 2018, "Optothermophoretic Manipulation of Colloidal Particles in Nonionic Liquids," J. Phys. Chem. C (epub).
[76] Lin, L., Peng, X., Wei, X., Mao, Z., Xie, C., and Zheng, Y., 2017, "Thermophoretic Tweezers for Low-Power and Versatile Manipulation of Biological Cells," ACS Nano, **11**(3), pp. 3147–3154.
[77] Lin, L., Wang, M., Peng, X., Lissek, E. N., Mao, Z., Scarabelli, L., Adkins, E., Coskun, S., Unalan, H. E., Korgel, B. A., Liz-Marzán, L. M., Florin, E.-L., and Zheng, Y., 2018, "Opto-Thermoelectric Nanotweezers," Nat. Photonics, **12**(4), pp. 195–201.
[78] Lin, L., Peng, X., Wang, M., Scarabelli, L., Mao, Z., Liz-Marzan, L. M., Becker, M. F., and Zheng, Y., 2016, "Light-Directed Reversible Assembly of Plasmonic Nanoparticles Using Plasmon-Enhanced Thermophoresis," ACS Nano, **10**(10), pp. 9659−−9668.
[79] Lin, L., Zhang, J., Peng, X., Wu, Z., Coughlan, A. C. H., Mao, Z., Bevan, M. A., and Zheng, Y., 2017, "Opto-Thermophoretic Assembly of Colloidal Matter," Sci. Adv., **3**(9), p. e1700458.
[80] Peng, X., Li, J., Lin, L., Liu, Y., and Zheng, Y., 2018, "Opto-Thermophoretic Manipulation and Construction of Colloidal Superstructures in Photocurable Hydrogels," ACS Appl. Nano Mater, **1**(8), pp. 3998–4004.
[81] Lin, L., Peng, X., and Zheng, Y., 2017, "Reconfigurable Opto-Thermoelectric Printing of Colloidal Particles," Chem. Commun., **53**(53), pp. 7357–7360.